Extended Methods for Robust Power System Topology Identification

Nicholas Piaquadio, N. Eva Wu, Ning Zhou
Department of Electrical and Computer Engineering
Binghamton University
Binghamton, New York 13902-6000
Email: {npiaqua1, evawu, ningzhou}@binghamton.edu

***Abstract*— New methods are proposed to continue to the development of a power system topology detection method designed for robustness under load uncertainty. The method maps load variation onto a space of measurements using the topology-dependent network model, then separates the mappings via convex optimization. Two new areas are explored. Statistical methods are applied to extend the detector's functionality to cases where an exact load uncertainty set cannot be established, and tested on the IEEE 9-bus system. The use of Support Vector Classifiers allows a detector of specified accuracy to be established when the load uncertainty sets are not strictly separable. In the second half of the paper, the original formulation is re-worked to allow its application to larger power networks, and is demonstrated on the IEEE 68-bus system. A placement rule is proposed for additional sensors.**

I. INTRODUCTION

This paper seeks to develop a secondary protective scheme to identify open circuit conditions independent of state estimation. The method is designed for robustness against load uncertainty, making it ideal for cases of high renewable penetration where distribution level generation may vary.

State-estimation based methods include measurement residual analysis as well as state vector augmentation [1]. Problems arise, however, in the case of bad or missing measurement data, or where the state estimation process does not converge. The missed detection of an opened line can lead to cascading outages as in the Southwest Blackout of 2011 [2]. State-estimation methods for fault identification furthermore rely on Supervisory Control and Data Acquisition (SCADA) system measurements. While widely available, SCADA measurements are not time-synchronized, and many do not record at regular intervals, or provide a time-stamp of when the measurement was taken [3].

Phasor Measurement Unit (PMU) measurements by contrast, are both high speed at 30-120 phasor measurements per second and time synchronized. While this provides an advantage over the SCADA system, PMUs are expensive, and as of 2017, only 2500 were operating in the North American Grid [4]. A Multiple Model Based (MMB) approach to topology identification can help this problem, by classifying a minimal set of PMU measurements to the nearest model. A direct example is found in [5], where open-circuit topology detection was performed using time-series PMU data, classifying topology by finding the closest model in a 2-norm sense.

For open circuits, slower dynamics allow the use of phasor-domain analysis, simplifying the computational process. A toplogy identification method based on phasor angles was proposed in [6], comparing the measured angles at several PMU points with the model for each topology and taking the closest. Angles were also applied in [7], which used a machine-learning methodology based on historical data. The authors in [8] used the 2-norm between phasor current measurements, then determined limits on load variation beyond which the detector would be inaccurate. Open circuit identification methods also find application in islanding detection [9].

For an open circuit detector, two main concerns are isolability, the ability to distinguish as many lines as possible, and robustness, the capacity to correctly identify open circuits in the presence of modeling error [10]. All the aforementioned works achieve isolability, but only [8] discussed robustness. The consideration of load uncertainty as the primary source of modeling error is of particular interest as renewable penetration increases at the distribution level, making the load change with weather conditions.

This paper is a direct extension to prior work [11] that sought to address this robustness issue for topology detection. In that paper, load uncertainty was modeled as a current injection at the load points. The possible values of this injection exist within a set, called the load uncertainty set. A convex set in the form of a hyperrecctangle was constructed to contain the load uncertainty set. The hyperrecangles were mapped onto the measurements via affine transformations, defined by the circuit model of the network, and unique for each open circuit topology. Set separability was checked by solving the separating hyperplane problem for polygons [12].

The mappings of the load uncertainty set define the reachable set of outputs under each topology. Therefore, if the sets intersect for two topologies, they cannot be distinguished assuming the real load matches the load uncertainty set. An algorithm was developed to find the maximum tolerable load uncertainty for a given set of measurements and tested on the IEEE 9-bus system using phasor measurements of each generator current.

In this work, an alernative point based method is developed for topology detection, and the original algorithm is expanded for larger power systems, and demonstrated on the IEEE 68-bus test system. Rather than parameterize load uncertainty as a convex set, the particular load current is

considered to be a point drawn from a random distribution. This may be useful in the case where there is little data available, but a variance has been established. It furthermore allows the application of a support vector classifier (SVC) to minimize misclassification in practical cases where the reachable sets under two topologies do overlap.

The original algorithm in [11] is furthermore extended to include voltage measurements, and to consider load points at the generator terminal busses. A placement rule for new measurements is developed to maximize sensitivity to a particular change in topology while minimizing sensitivity to load variation. With extra measurements in place, the detector's performance is assessed fitting the load uncertainty set within a uniform hypercube, and a euclidean norm ball.

The rest of the paper is outlined as follows. Section II provides background on the formulation of the detector. Section III develops the point-based statistical method for topology detection, and aaplies it tomthe IEEE 9-bus system. Section IV extends the original convex set-based algorithm to the 68 bus system with numerical results. Section V discusses the remaining practical concerns for the implementation of the extended method, and Section VI contains the conclusions drawn from the work.

II. DETECTOR FORMULATION

The problem setup for the detector follows the previous work in [11], but drops the assumption that there are no loads at the generator terminals, allowing application to more systems.

The power system model used for this problem assumes the network to be in a quasi-steady state sinusoidal (QSSS) state [13], so the generators are modeled as an ideal voltage source behind an impedance, removing transient effects. Loads are modeled as a nominal admittance, while load uncertainty is considered as a uncertainty in injected current at the load busses as shown in Figure 1.

The nominal currents are first solved from the admittance matrix for each of the contingent topologies [14]. In the nine-bus case, the detected topologies are: $\{00, 45, 46, 57, 69, 78, 89\}$, indexed in terms of the opened line, with 00 representing the in-tact case.

The admittance matrix also defines the mapping between the uncertain load currents, which will be called the Load uncertainty Space, and the measured generator currents, which will be used by the detector, and is therefore dubbed the Decision Space:

$$\begin{aligned}\begin{bmatrix} I_g^{nom} \\ V_t^{nom} \\ V_l^{nom} \end{bmatrix}^k + \begin{bmatrix} \Delta I_g \\ \Delta V_t \\ \Delta V_l \end{bmatrix}^k &= M^{-k}(L_{nom}^k + \Delta L^k) \\ &= \begin{bmatrix} I & Y_{gg} & 0 \\ 0 & Y_{tt} & Y_{tl} \\ 0 & Y_{lt} & Y_{ll} \end{bmatrix}^k \setminus \left(\begin{bmatrix} Y_{gg}E' \\ Y_{gg}E' \\ 0 \end{bmatrix}^k + \begin{bmatrix} 0 \\ \Delta I_t \\ \Delta I_l \end{bmatrix}^k \right)\end{aligned} \tag{1}$$

Here, $\{I_g, I_t, I_l\}$ are the currents at the generators, terminals, and load busses respectively, E' is a vector of the internal EMFs, V_t, and V_l are the voltages at the terminal and load busses, and $\{Y_{gg}, Y_{tt}, Y_{tl}, Y_{ll}\}$ are the admittance matrix entries between the generator busses, between the terminal busses, from terminal to load, and between the load busses. The superscript k represents that each of these quantities is dependent on the topology of the network.

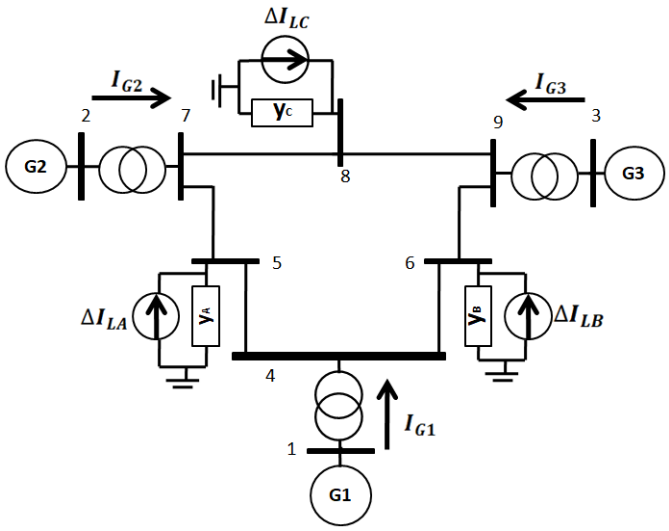

Fig. 1. One line diagram of the IEEE 9-bus test system [15]. The system is redrawn to show the nominal load admitance and variation as a perubation in load current. PMU data are assumed available at the generator terminal buses 4, 7, and 9. Buses 5, 6, and 8 have nominal loads A, B, and C, respectively.

This formulation explicitly separates the nominal components, caused by the EMF sources, and the uncertainty components, caused by injection due to load variation. The possible measurements are drawn from the set $\{I_g, V_t, V_l\}$. In short-hand, the block admittance matrix is M^k, the vector from the generator sources is L_{nom}^k and the uncertainty vector is ΔL^k

Let $\Delta\ell$ correspond to the real-valued uncertainty vector containing all the rectangular components of the load currents: $\Delta\ell = [Re\{\Delta L\}\ ,\ Im\{\Delta L\}]'$

Then, since M^k represents the admittance matrix in the form from (1), this gives Δd, the change in the decision space of real-valued measured variables as the following:

$$\Delta d^k = \begin{bmatrix} Re\{M^{-k}\} & -Im\{M^{-k}\} \\ Im\{M^{-k}\} & Re\{M^{-k}\} \end{bmatrix} \Delta\ell = F^k \Delta\ell. \tag{2}$$

Here, the topology-dependent matrix F^k is the real-valued inverse of M, and defines a linear mapping between load uncertainty and measurement uncertainty.

To define a set of load uncertaintys, a hypperectangle, R, was generated in terms of hyperplanes, such that $\Delta\ell \in R$ implies that $A^t\Delta\ell \preceq b$. The load uncertainty hypperrectangle translates to the decision space via an affine transformation:

$$D^k = F^k R + d_{nom}^k \tag{3}$$

Where d_{nom}^k is the nominal measurement under topology k. This mapping makes one polygon, D, for every topology,

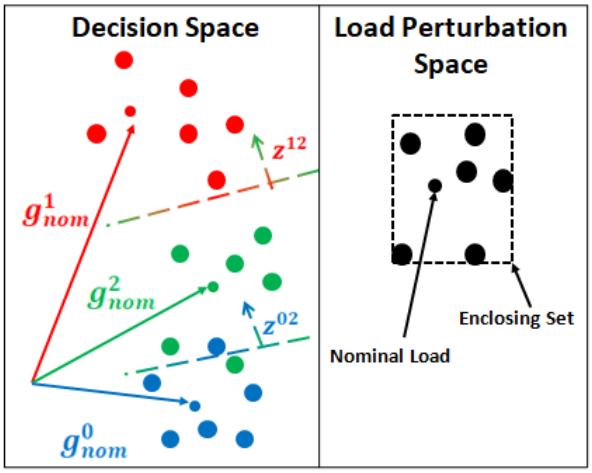

Fig. 2. Conceptual illustration of the mapping between the uncertain load current variation, and the corresponding points in decision space based on measured values. The Load Uncertainty Set belongs to a convex feasible set that may or may not be known. Three mappings are applied to place the sampled load variation onto different topologies. Pairs 0-1 and 0-2 are strictly separable, while pair 1-2 has overlap, and necessitates a detector with some error rate.

k. If the D^k do not overlap, then each possible measurement vector belongs to a unique topology, and an error-free detector can be established with guaranteed robustness for any uncertainty within R.

Choosing to represent the load uncertainty as a hyper-rectangle means that it is a convex set, and under affine transformation, remains convex. As such, the separability of D^k can be checked by solving the separating hyperplane problem for polyhedra [12]. Further details on the algorithm are contained in [11].

III. DISCRETE POINT DETECTION APPROACH

In this section, point-based methods are developed for robust open circuit topology detection and applied to the IEEE 9-bus system.

A. Point-Based Problem

Considering the load uncertainty set to be a set of points, the problem of topology detection is the classify the mapped points according to what topology they originated from. Applying the mapping in (2), a single load point, $\Delta\ell$ maps to a single decision space point d, as $d^k = F^k\Delta\ell + d^k_{nom}$, mapping using the matrix F, then adding the nominal. The new problem is to define a detector that discriminates between these mapped sets, which may overlap.

To achieve this, a separating hyperplane is drawn between the points sampled from each topology, or as close as possible if the feasible sets in two distinct topologies overlap. Figure 2 demonstrates this mapping process, as well as the use of the separating hyperplanes.

For the case where the samples from each topology are not strictly separable, some level of mis-classification must be allowed. In this case, a support vector classifier [12] is applied to the problem , trading off the sum least squares distance of each mis-classified point to the hyperplane with the size of the slab containing all mis-classified points. This slab width parameter is an important aspect of robustness: a larger region means the classified sets are more separated. Because the problem is scalarized multi-criterion, adjusting the scalar weighting factor γ allows several candidate detectors to be explored.

(4) expresses this problem for all topology pairs a and b, where D_a is the set of points in topology a and D_b is the set of points in topology b.

$$\begin{aligned} &minimize \quad ||z||_2 + \gamma \sum_i (u[i] + v[i]) \\ &subject\ to \\ &\qquad z^T D_a[i] - c \geq 1 - u[i], \ \ \forall\, i \\ &\qquad z^T D_b[i] - c \leq -(1 - v[i]), \ \forall\, i \\ &\qquad u \succeq 0, v \succeq 0 \\ &\qquad for\ all \quad a, b \in k, \ a \neq b \end{aligned} \tag{4}$$

Here, the variables are u, v, z and c. z is a six-vector for the 9-bus system since there are six generator current components in the decision space and c is a scalar. The u and v vectors each have a single element for each point sampled, so their size is equal to the number of samples used. The parameters are D_a and D_b, and are sets of randomly or non-randomly sampled points from the two topologies. The problem is solved between each topology, pair, dictated by the last statement in the problem.

B. Application to 9-bus System

For the 9-bus system case, PMU generator current measurements are taken at the high side terminals of each generator. By superposition, each measured generator current can be separated in to the nominal component without the load current uncertainty, $I^k_{g\,nom}$ and a uncertainty component caused exclusively by the load current uncertainty, ΔI_g. As in[11], this simplifies the detector formulation somewhat, since the 9-bus system has 3 generators and 3 loads, meaning the load uncertainty space and decision space are both 6-dimensional.

To verify the operation of the method, the hyperrectangular load uncertainty found in [11] of 0.21 pu at all load current components was first checked. To do this, instead of experessing the hyperrectangles as facets, the vertices were taken as a set of discrete points. Mapped to the decision space, then, if the hyperrectangles do not overlap, the sets of vertices should be strictly separable.

This condition can be checked using (4), whereas, if no points are misclassified, then vectors u and v are the zero-vector. Hence, if the problem with u and v set to zero, or the robust classifier problem [12] is feasible, then the hyperrectangles are strictly separable.

For the IEEE 9-bus system, using the vertices was slightly faster than the original formulation considered in [11], taking 5.49 seconds as opposed to 5.68 to check separability. Both algorithms were implemented in MATLAB on a 3 GHz

8 core processor using the CVX toolbox for disciplined convex programming [16] However, the size of the problem grows exponentially with the number of loads as the load uncertainty set grows in dimension, whereas the original facet formulation grows linearly. Therefore, considering the sets as a collection of vertices is only useful for small systems or as verification.

The more interesting use case for this method occurs when the load variation is not exactly known, but a sample dataset has been collected. For this purpose, several samples of 10,000 load points were generated in the load uncertainty case under two cases. First a uniform in each current component. Setting the limit of the uniform variation past 0.21 pu induces points outside the tolerable set, with the error rate determined by how far the variation extends beyond that limit. These points are mapped into each of the 7 potential topologies, then separated using 4. Varying the scalarizing parameter γ trades off detector accuracy on this 70,000 point set with the slab length, or robustness of the detector, in units of measured generator current per-unit.

Table I shows the results under 0.24 pu of uniform variation in all components. For this random sample, 16 points are found inseparable under any detector. Each separation problem contains two samples of 10,000 points, and there are 21 pairs, so there are 420,000 total scalar constraints in the problem in the form of (4). The percentage of non-zero entries in the u and v vectora provides the error rate is. While a higher gamma always corresponds to better accuracy, the smaller magnitude of z means the slab width, or separation, is small, corresponding to overfitting on the provided sample, and potentially worse real-world performance.

TABLE I
DETECTORS FOR UNIFORM 0.24 PU LOAD VARIATION

gamma	10000	10	1	0.5
Mean Slab Width (pu)	0.2862	0.2943	0.3201	0.3438
Errors	16	33	170	338
Error Rate (%)	0.0038	0.0078	0.0402	0.08
gamma	0.05	0.01	0.005	0.001
Mean Slab Width (pu)	0.4553	0.4783	0.4909	0.5353
Errors	2635	11783	22587	100664
Error Rate (%)	0.6234	2.7876	5.3437	23.8152

The second distribution was gaussian. In a practical sense, the guassian distribution has the desirable property that points will be concentrated around the center, with rare outliers. The rate of outliers is controlled by the covariance of the multivariate distribution. These points were generated according to the following probability distribution:

$$\kappa(\Delta\ell, \Sigma) = \frac{1}{(2\pi)^3 \Sigma^{1/2}} e^{-\frac{1}{2}\Delta\ell\Sigma^{-1}\Delta\ell} \tag{5}$$

Here, the probability density κ for a particular load variation $\Delta\ell$ follows a standard multi-variate gaussian distribution in six dimensions, with covariance matrix Σ. For this experiment, 10,000 points were sampled in load uncertainty space using the conservative assumption that the load current components are uncorrelated, reducing Σ to a diagonal matrix.

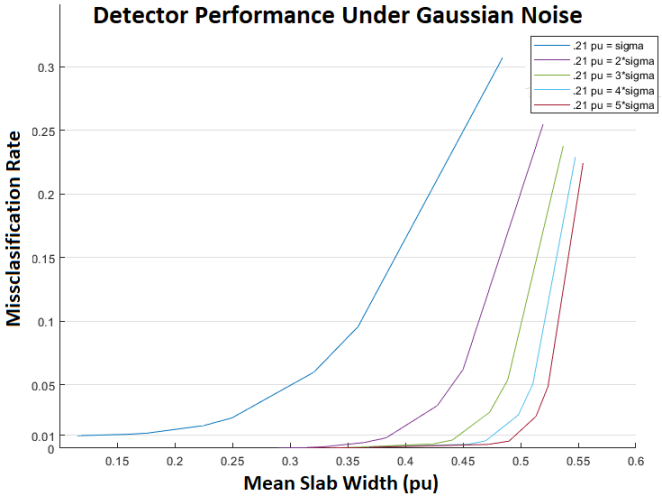

Fig. 3. Error rate vs detector robustness for several levels of uniform gaussian load variation. In this case, the optimum detector is at the bottom right, as more slab width and few errors are both desirable. Notably, when the uniform deviation is two standard deviations for the uncertainty, the error rate can be made arbitrarily small for the 10,000 point sample used.

An optimal trade off curve was established by varying γ under several levels of uniform noise. Since the absolute limit on the hyperrectangular load uncertainty set is 0.21 pu for perfect detection [11], setting the standard deviation to 0.21 pu means each boundary has a 31.74 percent chance to be broken. Then, setting 0.21 a multiple of the standard deviation pushes errors further out on the normal distribution. The problem (4) was solved with 0.21 pu equal to one standard deviation up to five standard deviations.

The resulting tradeoff curves in Figure 3 show that if the absolute set boundary is two standard deviations for the uncertainty, the detector can be made highly accurate without sacrificing too much in the way of slab width. In particular, even where the limit for perfect detection is only one standard deviation, finding a point that actually gets misclassified is fairly rare, close to 1 percent, while at two standard deviations the error rate can be pushed near zero. This provides an important link between the set boundary established in [11], and real world systems, whereas if two standard deviations of the real variation is tolerable as hypercube, strong detector performance can be assured.

IV. EXTENSION TO LARGER SYSTEMS

In this section, the-set based topology detection method described in [11] is generalized to large power networks, and a rule for sensor placement is proposed.

For an open circuit detector to work, it must be able to both detect all possible open circuit conditions, as well as identify the particular line that has been opened. Achieving detectability and identifiability without load uncertainty is a necessary prerequisite to the robust detector design.

Suppose S is the set of all possible open-circuit topologies, and the topologies are considered in pairs, $k, m \in S$. Then, detectability can be defined as follows:

$$||p^0_{nom} - p^k_{nom}|| \geq \epsilon > 0, \ \forall \ k \in S \tag{6}$$

Here, p^i_{nom} represents the nominal (no load change) measurement vector under topology i, and 0 is the in-tact case. Idenfitiability imposes the further requirement that all topology pairs are distinguishable by at least ϵ:

$$||p^m_{nom} - p^k_{nom}|| \geq \epsilon > 0, \ \forall \ k, m \in S \tag{7}$$

In a perfect system, any epsilon greater than zero is sufficient to establish identifiability, however, in practice, it is desirable to have as large an epsilon as possible to provide a margin against measurement and modeling error. In terms of load uncertainty, raising the identifiability means the decision space is more sensitive to topology change, allowing a greater amoung of uncertainty to be tolerated.

For a specified level of identifiability, ϵ, it is desirable to find the minimal set of additional sensors added to the system. Suppose there are P existing scalar measurements in the system. An additional PMU adds a real component, a and and imaginary measurement component b , and there are N possible sensors. The goal is to raise the identifiability between all possible topology pairs, k and m. Adding measurements cannot decrease the identifiability, so only those pairs that violate the inequality for ϵ need to be considered. Allowing this set to be S_{iden}, the following linear program provides an optimal placement rule:

$$\begin{aligned}
&minimize \quad \sigma_1 + \sigma_2 + ... + \sigma_N \\
&subject\ to: \\
&0 \leq \sigma_i \leq 1 \\
&\sum_{i=1}^{P} (p^k_i - p^m_i)^2 + \sum_{i=1}^{N} \sigma_i [(a^k_i - a^m_i)^2 + (b^k_i - b^m_i)^2] \geq \epsilon^2 \\
&for\ all\ pairs \ \ k, m \in S_{iden}, k \neq m
\end{aligned} \tag{8}$$

Here, the objective is the sum of the placement variable σ_i, for each sensor, which is relaxed from a binary variable to the range [0,1], making the problem a linear program rather than a mixed-integer program. Given a set of σ_i values, the placement solution is obtained by rounding each to zero or one, then checking the placement against the target value for ϵ.

To test the performance of this placement method with the original convex algorithm in [11], it was applied to the IEEE 68 Bus system, shown in Figure 4. Notably, the 68 bus 16 machine system has 35 load points, and will require more measurements so both the load uncertainty and decision spaces are much higher dimension than for the 9 bus system.

For the 68 bus system, some of the lines are not n-1 secure, whereas the system is not stable under their removal [17]. Without these, there are 50 open circuit topologies

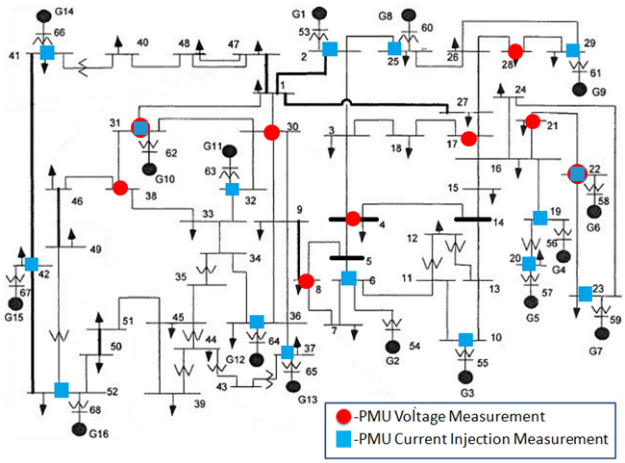

Fig. 4. One Line Diagram of IEEE 68 Bus Test System [18]. The measurements placed for this study are indicated on their corresponding bus, while inter-area tie lines are indicated with a thicker connecting line. The initial measurements were the generator currents (blue squares), with six voltage measurements added.

left to detect. To begin, as in the 9-bus case, PMU current measurements were placed at the terminal busses of each generator. In this case, the detectability ϵ was 0.1036, while identifiability was 0.0898. With voltage measurements added at every bus, detectability only increases to 0.1465, and identifiabiltiy to 0.1233.

These values are a bit low for the purposed of robust detection. After some observation, three lines were identified: 1-27, 3-18 and 31-38, that have near-zero current values in the nominal case. Openint these lines causes only a small change in power flow, making their topology change difficult to detect. Table II summarizes the increase in potential epsilon values:

TABLE II

DETECTABILITY AND ISOLABILITY OF THE 68 BUS SYSTEM

Case	All Lines	3 Lines Not Considered
Detectability ϵ (pu)	0.1036	0.1772
Identifiability ϵ (pu)	0.0868	0.1592
All Sensors Detectability ϵ (pu)	0.1465	0.2521
All Sensors Identifiability ϵ (pu)	0.1233	0.2291
Size of Tolerable Hypercube (pu)	0.01	0.15

Given this benefit, for the purpose of design, the three topologies are not considered, and are left to be handled separately, for example, by direct current measurement. This leaves 46 total open circuits and the nominal, or 47 topologies to be detected. The problem 7 was solved for an identifiability of 0.22, near the maximum, with σ values greater than 0.3 rounded to 1. The eight sensors identified in red in Figure 4 represent this placement solution.

In terms of performance, the 22 sensor scheme in Figure 4 completes the algorithm described in [11] with a time of 247 seconds, tolerating 0.15 pu of load variation at all points. Since a hyperectangle was used, this value comes in the sense

of an infinity more, so all components of all load currents can change by 0.15 pu, and a perfect detector can still be established. By comparison, changing the uncertain set to a 2-norm ball causes the algorithm to take 358 seconds to run, and finds 0.28 pu of load uncertainty to be tolerable. In this case, however, the uncertain set allows large variation in one component only if the others are comparatively close to nominal.

Once the hyperplanes have been established, checking the topology of a given measurement takes an average of 817 μs. This is considerably slower than the 9 bus system at 161 us [11], but is still about 20 times faster than a single 60Hz cycle, meaning the detector is more than fast enough for on-line operation.

V. DISCUSSION

The statistical methods demonstrated establish a useful connection between the set-based uncertainty limit and the variance of the load, namely, that the limit should be at least two standard deviations for good performance. Measurement noise can be added to the method by adding an additional random factor to the points post-mapping. One issue is the problem size, since each topology pair must be separated, and each point adds a scalar variable to the SVC problem. This makes detailed Monte-Carlo type analysis computationally costly.

The extended method applied to the 68 bus system faces a few barriers to practical implementation. Foremost, lines with little power flow in the nominal case are nearly unobservable, since the power flow in the network changes only slightly with them removed. A direct measurement of the line current solves the issue, since it will be zero with the line removed, however, it wouldn't be feasible to add PMU measurements for every line current.

As far as finding the tolerable load uncertainty, the high dimensionality of the 68-bus system, at 44 scalar measurements and 70 scalar uncertain parameters causes a long desgin time at 4-6 minutes, compared to 5.66 seconds for the 9-bus system, with 6 scalar measurement and 6 parameters. This means the detector design is presently too slow to keep up with the load forecast in real time, but the online operation remains fast at 817 μs to check the current topology.

As may be expected. the suggested placement rule often selects measurements on the end-points of line i or j, when trying to separate topology i and j. It may also be desirable to find a single measurement that best separates two or more distinct pairs, in which case the average of the objectives can be applied.

VI. CONCLUSIONS

The extended methods in this work extend the original multiple model based detector to operate on larger test systems and in scenarios where strict separation of the decision-space reachable sets is not possible.

Considering load uncertainty as a random distribution rather than a set opens new types of analysis for the topology detector and provides a meaningful connection between known variance and hard set limits. A re-formulation allows the original convex techniques to apply to power systems of arbitrary size, though the 68 bus system highlights the increasing cost in terms of design time as the convex problems grow in size.

Future work in this are may include methods to handle lines with low power flow, and hence weak detectability. In addition, in place of a hyperrectangle, uncertain distribution or norm ball, a practical approach would be to wrap a confidence ellipsoid around real load data or an accurate load model, then perform separation.

REFERENCES

[1] A. Abur and A. G. Exposito, *Power System State Estimation Theory and Implementation*. Marcel Dekker, 2004.

[2] "Arizona-southern california outages on september 8, 2011: Causes and recommendations," *Federal Energy Regulatory Comission, Washington, DC, USA and North American Electric Reliability Council, Atlanta, GA, USA, Tech. Rep.,*, 2012.

[3] X. Ma, C. Liu, J. Wu, and C. Long, "On-demand state estimation with sampling time skew in power systems," *2015 IEEE Canadian Conference on Electrican and Computer Engineering*, 2015.

[4] A. Silverstein, "Synchophasors and the grid," *North American SynchroPhasor Initiative, Tech. Rep. NARUC Summer Meeting*, 2017.

[5] G. Cavraro and R. Arghandeh, "Power distribution network topology detection with time-series signature verification method," *IEEE Transactions on Power Systems*, vol. PP, pp. 1–1, 12 2017.

[6] J. Tate and T. Overbye, "Line outage detection using phasor angle measurements," *Power Systems, IEEE Transactions on*, vol. 23, pp. 1644 – 1652, 12 2008.

[7] J. He, M. X. Cheng, Y. Fang, and M. L. Crow, "A machine learning approach for line outage identification in power systems," in *Machine Learning, Optimization, and Data Science*, (Cham), pp. 482–493, Springer International Publishing, 2019.

[8] M. Sarailoo and N. E. Wu, "Maximum tolerance to load uncertainty of a multiple model based topology detector," *IEEE Power and Energy Society General Meeting (PESGM)*, 2020.

[9] M. Salman and N. E. Wu, "Islanding detection in electric distribution circuits using multiple-model filters in the presence of multiple pv inverters," *in 2019 American Control Conference (ACC)*, pp. 3174–3179, 2019.

[10] J. Gertler, "Survey of model-based failure detection and isolation in complex plants," *IEEE Control Systems Magazine*, 1988.

[11] N. Piaquadio and N. E. Wu, "Robust topology detection under load uncertainty," *American Control Conference*, 2021.

[12] S. Boyd and L. Vandenberghe, *Convex Optimization*. Cambridge University Press, 2009.

[13] M. Sarailoo, N. E. Wu, and J. Bay, "Transient stability asessment of large lossy power systems," *IET Generation, Transmission Distribution*, 2018.

[14] H. Saadat, *Power system analysis*. WCB/McGraw-Hill, 1999.

[15] P. M. Anderson and A. A. Fouad, *Power system control and stability*. John Wiley & Sons, 2008.

[16] CVX Research, "CVX: Matlab software for disciplined convex programming," Version 2.2, January 2020, http://cvxr.com/cvx/.

[17] N. E. Wu, M. Sarailoo, and M. Salman, "Transmission fault diagnosis with sensor-localized filter models for complexity reduction," *IEEE transactions on smart grid*, 2018.

[18] R. A. Ramos, R. Kuiva, T. C. Fernandes, L. C. Pataca, and M. R. Mansour, "IEEE PES task force on benchmark systems for stability controls," *Pac. Northwest Nat. Lab, Richaland, WA, USA*.